Andean Geology 50 (2): 269-290. May, 2023
doi: 10.5027/andgeoV50n2-3450

Andean Geology
www.andeangeology.cl

Diagenesis of continental carbonates linked to the evolution of the flexural margin of the Triassic Sorocayense-Hilario rift sub-basin, Argentina

***Cecilia Andrea Benavente[1, 2], Sergio Matheos[3], Silvia Barredo[4], Fernando Abarzúa[5], Adriana Cecilia Mancuso[1]**

[1] *Instituto Argentino de Nivología, Glaciología y Ciencias Ambientales (IANIGLA), CCT-Mendoza, CONICET, Av. Adrián Ruiz Leal s/n, Parque General San Martín CC 330 (CP 5500) Mendoza, Argentina.*
cebenavente@gmail.com, amancu@mendoza-conicet.gob.ar

[2] *Geología, Facultad de Ciencias Exactas y Naturales (FCEN), Universidad Nacional de Cuyo (UNCuyo), Mendoza, Argentina.*

[3] *YPF Tecnología (YTEC), CONICET, Av. del Petróleo s/n, Berisso 1923, Buenos Aires, Argentina.*
sergio.matheos@ypftecnologia.com

[4] *Instituto del Gas y del Petróleo (IGPUBA), Av. Las Heras 2214, piso 3, Buenos Aires, Argentina.*
silviabarredo@yahoo.com

[5] *Sold Gold Plc, Av. Coruña E25-58 y San Ignacio, Edificio Altana Plaza, piso 4, oficina 406, Quito, Ecuador.*
fabarzua@solgoldecuador.com

**Corresponding author: cebenavente@gmail.com*

ABSTRACT. The lithostratigraphic units that conform the Sorocayense Group and fill the Sorocayense-Hilario sub-basin represent an alluvial-fluvial-lacustrine succession with significant volcanic supply during its deposition. They are namely the Cerro Colorado del Cementerio, Agua de los Pajaritos, Monina, Hilario and El Alcázar formations and present several carbonate levels. The genesis, diagenesis, and main controlling factors on continental carbonates present a means to understand basin evolution through the study of their petrography and chemical elemental composition through cathodoluminescence techniques. We have identified six microfacies: a) homogeneous micrite, b) bioclastic micrite, c) dolomicrite, d) laminated micrite, e) oncolitic packstone, and f) sparitic carbonate. Among these microfacies, six cementation and alteration phases have been identified: a) micritization, b) mechanical compaction, c) calcitic cementation, d) sparitic cementation, e) microsparitic cementation, and f) chemical compaction. This analysis allowed establishing a chronology of the diagenetic modifications undergone by the carbonates. Results support diagenesis was controlled mainly by tectonics showing major impact in carbonate facies identified at the flexural margin of the rift. The effect would have been linked to exertion of a paleohydrological effect favoring lateral meteoric water migration through faulting. The presence of dolomite in some of the microfacies is linked to the presence of montmorillonite as the dominant Mg-rich-phyllosilicate in clay assemblages most likely acting as the potential source. In turn, Mg is more likely to be replaced by Mn leading to luminescent carbonate microfacies.

Keywords: Lacustrine, Cathodoluminescence, Petrography, Rift, Middle Triassic.

RESUMEN. Diagénesis de los carbonatos continentales del margen flexural de la subcuenca Sorocayense-Hilario, Argentina. Las unidades litoestratigráficas que conforman el Grupo Sorocayense y que constituyen el relleno de la subcuenca Sorocayense-Hilario representan sistemas aluviales-fluviales-lacustres con aporte volcánico significativo durante su depositación. Estas unidades corresponden a las formaciones: Cerro Colorado del Cementerio, Agua de los Pajaritos, Monina, Hilario y El Alcázar y cada una de ellas contiene niveles carbonáticos. Estos carbonatos continentales constituyen un medio útil para entender la evolución de la subcuenca a través del estudio petrográfico complementado con técnicas de catodoluminiscencia. Estos estudios han permitido entender la génesis y diagénesis carbonática e inferir qué factores principales la controlaron. Se identificaron seis microfacies: a) micrita homogénea, b) micrita bioclástica,

c) dolomicrita, d) micrita laminada, e) *packstone* oncolítico, y f) carbonato esparítico. En tales microfacies, se identificaron seis fases de cementación y alteración: a) micritización, b) compactación mecánica, c) cementación calcítica, d) cementación esparítica, e) cementación microesparítica, y f) compactación química. Estos análisis permitieron establecer una cronología diagenética y apoyan la hipótesis de que la diagénesis fue controlada por la tectónica, con mayor impacto en las facies carbonáticas asociadas al margen flexural de la subcuenca. El principal efecto habría sido por medio de la acción paleohidrológica, lo que favoreció la migración lateral de agua meteórica a través de los fallamientos. La presencia de dolomita en algunas microfacies se vincula con la composición predominantemente montmorillonítica de los ensambles de arcillas que habría aportado el Mg. A su vez, en los carbonatos, el Mg tiende a ser fácilmente reemplazado por Mn, lo que causa incremento de la luminiscencia.

Palabras clave: Lacustre, Catodoluminiscencia, Petrografía, Rift, Triásico Medio.

1. Introduction

The Sorocayense-Hilario sub-basin is part of the Triassic Cuyana rift basin in western Argentina (Fig. 1). It has been thoroughly explored due to its rich fossiliferous content, mostly plant remains which have allowed to describe plant communities and to infer the paleoclimate (Spalletti, 2001; Bodnar *et al*., 2019; Ottone *et al*., 2019; Drovandi, 2020). The rocks of the Sorocayense Group are the main infill of the sub-basin, and despite the many structural, stratigraphical and sedimentological analysis of the area, the status of the Sorocayense Group units remains controversial (Baraldo and Guerstein, 1984; Abarzúa, 2016; Bodnar *et al*., 2019).

The Sorocayense Group is formed by five lithostratigraphic units that from base to top are: Cerro Colorado del Cementerio, Agua de los Pajaritos, Monina, Hilario and El Alcázar formations (Abarzúa, 2016; Bodnar *et al*., 2019). In the sub-basin, these units include several carbonate rock levels formed in different depositional settings ranging from floodplains of braided and meandering fluvial systems to a lacustrine margin, in the context of the passive margin of the northern half-graben of the Cuyana rift Basin at two localities, Quebrada del Agua de los Pajaritos and Quebrada El Alcázar (Fig. 1B). The development of the carbonate factory therefore spans different tectonic stages of the subbasin, from synrift to postrift in different tectonic settings, the active and the flexural margins of the rift (Abarzúa, 2016).

The main complexity for a clear stratigraphic definition for the lithological units of the sub-basin is the tectonic imprint that affected them through folding and faulting. All lithostratigrafic units host layers of carbonate rocks, which implies a broad time span for the carbonate deposition. Then, the study of their attributes could shed light on the diagenesis undergone by the whole sedimentary sequence and the nature of their principal drivers. Furthermore, characterizing the diagenesis of the carbonates has significant implications in different aspects such as the reconstruction and understating of the paleohydrology drainage patterns of the basin; and more applied aspects as well, such as the potential of the sedimentary rocks as a hydrocarbon source (Brigaud *et al*., 2009).

The aim of this study is to evaluate if the diagenetic stages recorded in the continental carbonates of the Triassic Sorocayense Group rocks were controlled by the tectonic active phases of the rift. For this purpose we used a detailed microfacies study and cold-cathodoluminescence analysis of carbonate rocks outcropping at the Sorocayense-Hilario sub-basin in the Quebrada del Agua de los Pajaritos and Quebrada El Alcázar localities (Fig. 1B). Such studies are relevant since the tectonic history of basins determines the diagenetic trends of the deposits (Grover and Read, 1983).

2. Geological setting

The Cuyana Basin is the largest Triassic rift basin of western Argentina (Fig. 1A) and is considered to extend over an area of more than 60,000 km^2. It corresponds to a continental rift (Ramos and Kay, 1991; Ramos, 2000; Legarreta *et al*., 1993; Barredo, 2004) developed as a consequence of the Gondwana Orogeny (Permian to Late Triassic-Early Jurassic) and the subsequent breakup of this supercontinent during Mesozoic times (Uliana and Biddle, 1988). It is composed of several asymmetric half-grabens (Fig. 1A).

The current geometry of the Cuyana Basin corresponds to a NNW-SSE elongate through with its margins affected by thrusts. Each sub-basin is bounded by mostly steeply deeping normal to oblique-slip faults that strike obliquely to the maximum

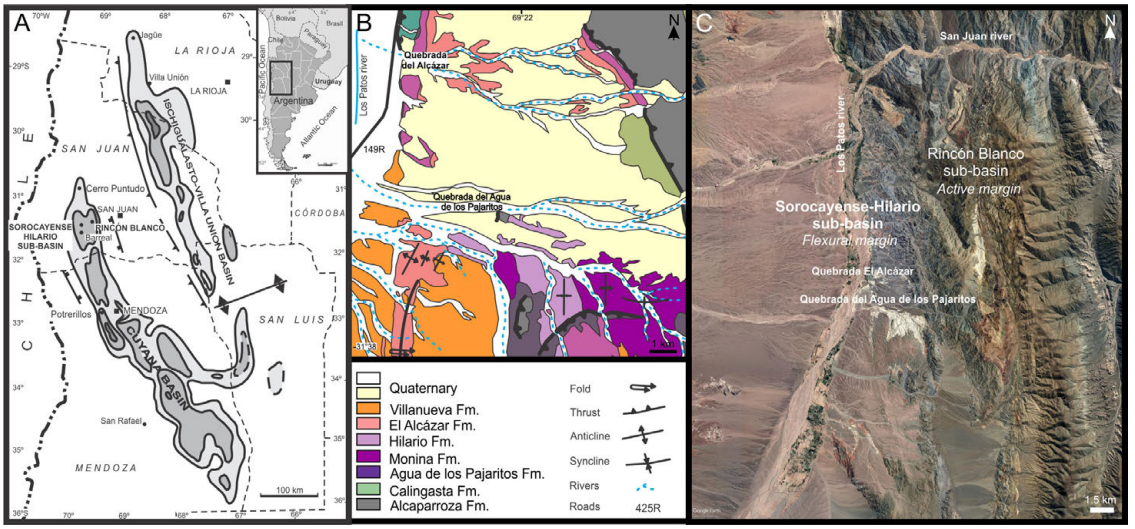

FIG. 1. **A.** Location map of the Sorocayense-Hilario sub-basin within the Cuyana rift Basin in the west-central region of Argentina showing the location of the master fault bounding the half grabens of the rift. Modified from Benavente *et al*. (2015). **B.** Geologic map of the Sorocayense-Hilario sub-basin of the Cuyana rift Basin. From Barredo *et al*. (2016). **C.** Location of the active and flexural margin of the Sorocayense-Hilario and Rincón Blanco sub-basins.

extension (Barredo, 2012). In detail, these border faults are segmented and have a stepped geometry with sometimes opposite dip directions (*e.g.*, Ramos and Kay, 1991; Legarreta *et al*., 1993; Barredo, 2004). Sub-basins correspond to asymmetric half-grabens separated by intrabasinal topographical highs that persisted throughout synrift and post-rift sedimentation keeping most of the troughs mostly isolated (Barredo *et al*., 2012; Abarzúa, 2016). This lack of physical connection between some of the sub-basins leads to different sedimentological conditions in their developments, especially in the Rincón Blanco sub-basin and Sorocayense-Hilario sub-basin, the focus of this study.

The Rincón Blanco and Sorocayense-Hilario sub-basins are located at 31°24'-31°33' south (Fig. 1A,B) conforming a narrow elongated half-graben (60 km N-S and 40 km wide) composed of different depocenters: Barreal, Agua de Los Pajaritos, and Rincón Blanco (Fig. 1A). The sedimentary deposits accumulated in the active margin of the half-graben (Rincón Blanco Group) reach more than 3,000 m in thickness and, today, present a geometry that consists of a north-south tight asymmetric syncline truncated by a series of west and east verging back-thrusts developed since Cenozoic times (Barredo, 2004; Abarzúa, 2016). The sedimentary rocks deposited on the flexural margin (Sorocayense Group) reach ~1,800 m in thickness and are represented by isolated outcrops currently separated from the active margin by a basement high. The Miocene Andean compression led to a positive basin inversion and a gently folding of the rocks formed in the ancient depocenters, in particular the Agua de Los Pajaritos one (Amos *et al*., 1971; Baraldo and Guerstein, 1984; Bonati *et al*., 2008; Abarzúa, 2016, among others) (Fig. 1B).

At the beginning of the Permian-Triassic extension the high strength of the crust led to the formation of a series of restricted half-grabens separated by intrabasinal highs and/or transfer faults (*e.g*., Ramos, 2000; Barredo, 2004; López Gamundí *et al*., 1994; Japas *et al*., 2008). The oldest sedimentary rocks correspond to the conglomerate and coarse-grained sandstone of the active margin of the sub-basin that built a narrow fringe of alluvial facies covered and interfingered with sandstone, siltstone and mudstone representing deposition in fluvial and lacustrine/playa-lake settings of the Rincón Blanco Group (Borrello and Cuerda, 1965; Stipanicic, 1979; Barredo and Stipanicic, 2002; Abarzúa, 2016).

In the flexural margin of the sub-basin, instead, the conglomerate, coarse-grained sandstone, siltstone and mudstone of the basin ill are represented by the Sorocayense Group (Stipanicic, 1972, 1979) distributed in two, separated depocenters (Fig. 1A).

2.1. The Sorocayense Group

The sedimentary rock succession in the Agua de Los Pajaritos depocenter on which this study is focused, are assigned to the Sorocayense Group composed of five lithostratigraphic units, with a thickness of 900 m, all of them bearing carbonate rock layers (Fig. 2). These units are from base to top the Agua de Los Pajaritos, Monina, Hilario and El Alcázar formations (Baraldo and Guerstein, 1984) (Figs. 2, 3A). The Agua de Los Pajaritos Formation is made up by conglomerates and coarse-grained

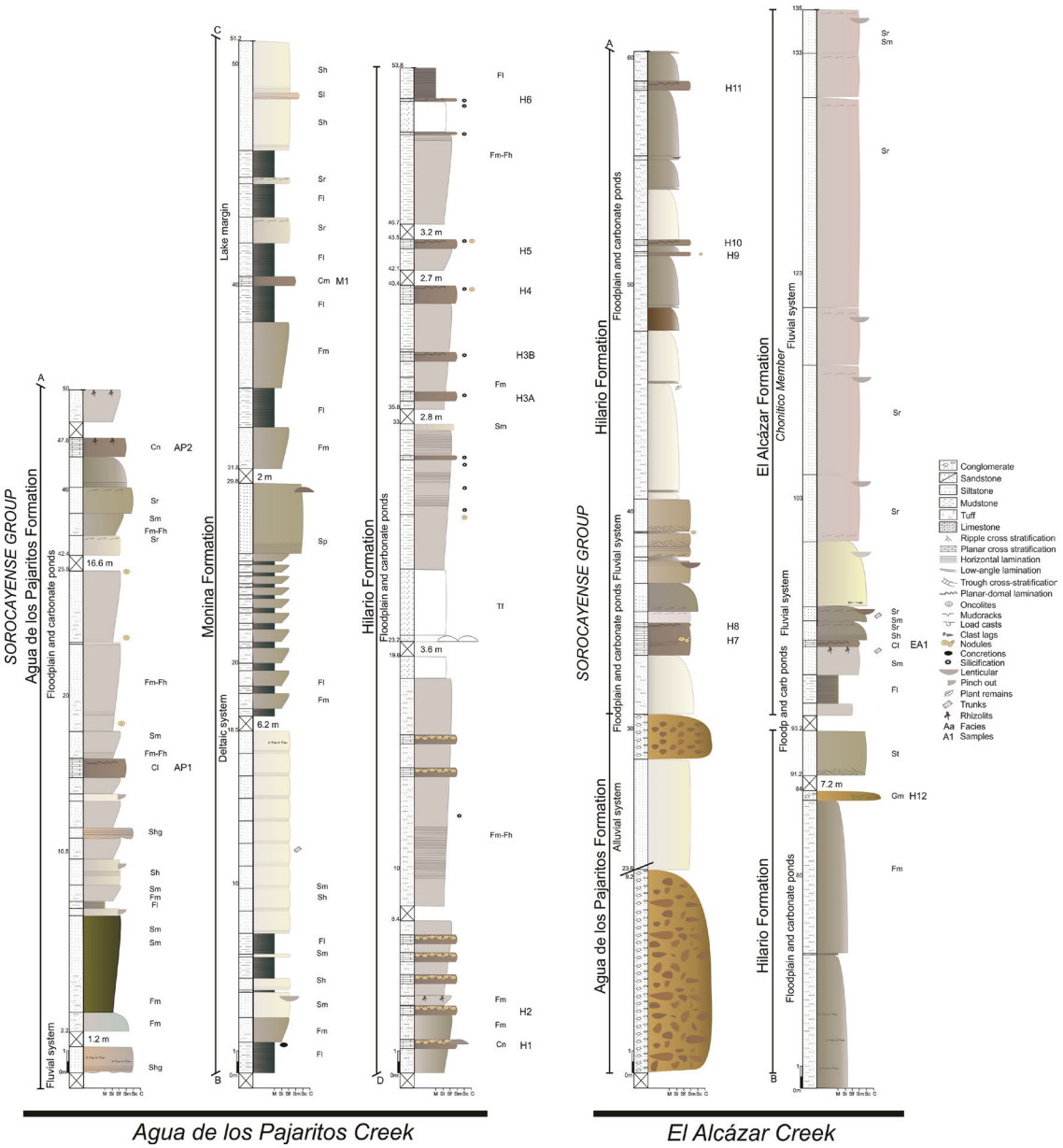

FIG. 2. High resolution sedimentary log of the Sorocayense Group (Agua de los Pajaritos, Monina, Hilario and El Alcázar formations) at the Quebrada del Agua de los Pajaritos and Quebrada El Alcázar creeks.

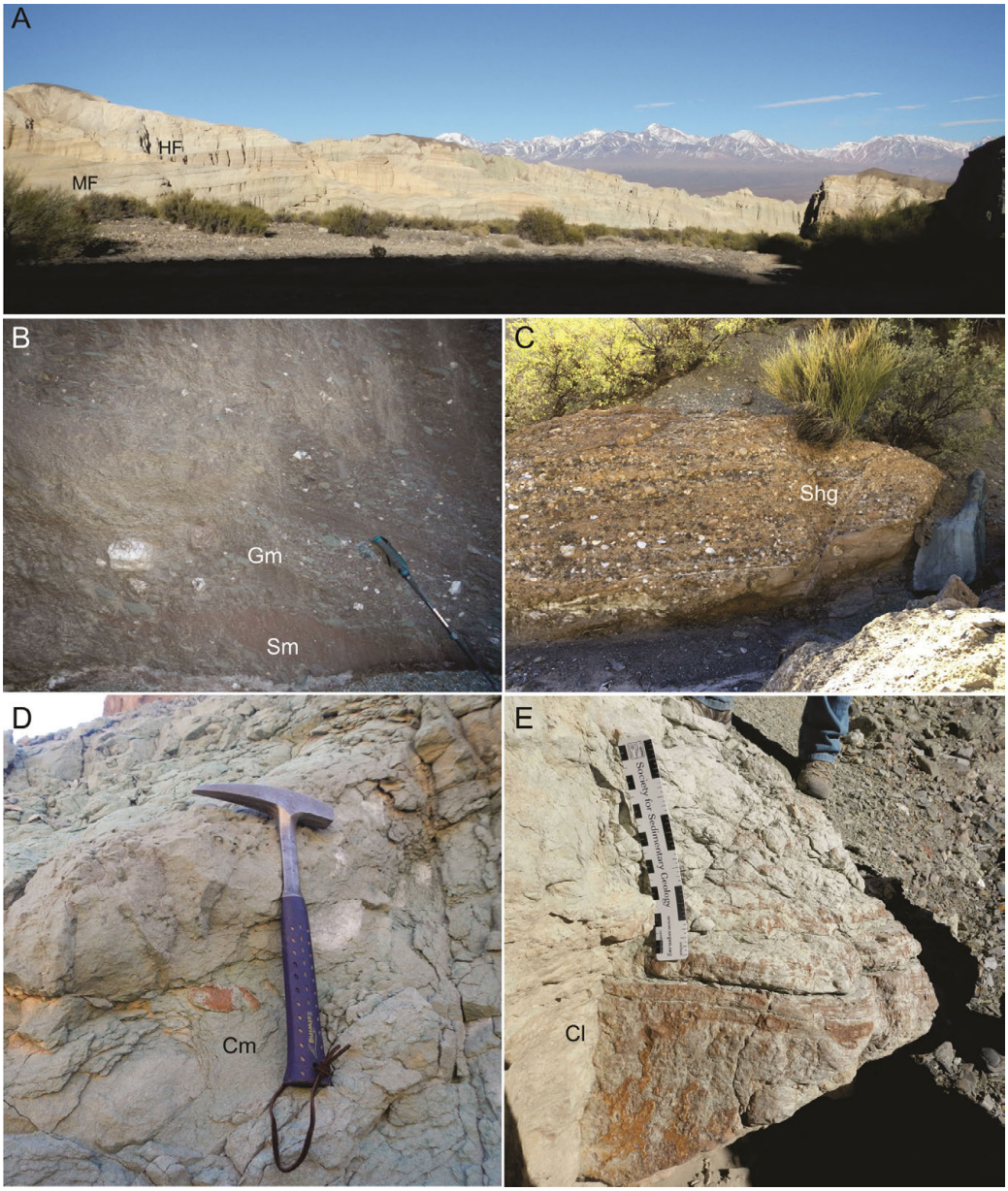

FIG. 3. Field photographs of the facies and facies associations of the Sorocayense Group and the Agua de los Pajaritos Formation. **A.** General view of the Monina and Hilario formations. **B.** Lithofacies Gm showing very poorly sorted, clast-supported, rounded and subangular pebble- to cobble-extraformational massive conglomerate interstratified with massive coarse-grained sandstone (Sm). Pole for scale is 1 m. **C.** Lithofacies Shg showing medium- to coarse-grained horizontally laminated sandstone with clast lags forming tabular to lenticular beds with erosive base. Scale is 25 cm. **D.** Cm lithofacies showing massive fabric with gleying and circular structures interpreted as rhizolithes. Hammer for scale is 35 cm. **E.** Carbonate bed representing the Cl lithofacies showing faint horizontal lamination in the base and nodules at the top. Scale is 10 cm.

sandstones that are grouped in a facies association (FA-A in Table 1), interpreted as debris flow deposited in an alluvial fan subenvironment (Table 1, Figs. 2, 3B); these lithofacies gradually passes upwards to medium-to coarse-grained sandstones (lithofacies Shg, Sh, Sr, Sm), which together constitute the

TABLE 1. SUMMARY OF THE FACIES ASSOCIATIONS OF THE SOROCAYENSE GROUP, SOROCAYENSE-HILARIO SUB-BASIN, CUYANA RIFT BASIN, ARGENTINA. MODIFIED FROM ABARZÚA (2016).

Formation	FA	Facies	Lithology	Structures	Bedding	Fossil Content	Lateral and vertical relationships	Interpretation
Agua de los Pajaritos	A	Gm	Moderate reddish orange (10R6/6) to pale red (10R6/2), very poorly sorted, clast-supported, rounded and subangular pebble- to cobble-extraformational conglomerate	Massive, matrix composed of medium-grained sandstone	Tabular, 2.5-23.6 m thick, extends laterally for several tens of meters, slightly erosional basal boundaries and planar upper boundaries	-	Overlies Alcaparrosa and Calingasta formations (Paleozoic) and Sm and underlies Sm, Sh-Shg and Fm-Fh	Debris flow, alluvial system
		Sm	Pale red (10R6/2), coarse-grained sandstone	Massive	Lenticular, 20 cm thick and extend for 1 m laterally	-	Underlies and overlies Gm	
	B	Shg	Grayish orange (10YR7/4), medium- to coarse-grained sandstone	Horizontally laminated, locally clast lags, clasts are subangular and 0.1-2 cm	Tabular, 0.1-1.4 m thick, erosive base	-	Overlies Fm and Shg and underlies	Tractive flows, fluvial system
		Sr	Medium- to coarse-grained sandstone	Ripple cross stratification. Sr: spacing is 1-5 cm, thickness is 0.5-1 cm	Tabular, 0.9-1.2 m thick	-	Overlies Sm and underlies Sh, Fm and Fh	
		Sm Sh	Dusky green (5G3/2), yellowish grey (5Y8/1), fine- to very fine-grained sandstone	Massive to faint horizontal lamination	Tabular, 0.3-3.3 m thick, pinch out laterally	-	Overlies Sh and Fm and underlies Sr	
	C	Fm	Very light grey (N8), yellowish gray (5Y8/1), light olive gray (5Y 6/1), very pale blue (5B8/2) siltstone	Massive to faint horizontal lamination, laterally silicified and/or nodular, nodules are 2-10 cm in diameter, clast lags, clasts are subrounded, 0.1 cm, mottling, mottles are 1 cm in diameter and bluish white (5B9/1), light blue (5B7/6) and pale purple (5P6/2) gleying	Beds are tabular and 0.2-3 m in thickness and persist laterally for hundreds of meters, and have non-erosional boundaries	Rhizolits with calcite infilling, 0.5-3 cm in diameter, concentric infilling	Overlies Sm, Sr and Cl and underlies Sm, Sr, Cl and Cn	Suspension settle out from waning flows, incipient paleosol development and fluctuating water table in the floodplain
		Cl	Very light grey (N8) color laminated carbonate	Planar lamination, 1 mm thick, laterally continuous, sparse domes	Tabular, 0.8 m thick	Ostracods Oncolites	Overlies Fm, Cn, Sm and underlies Sh	Subaqueous calcium carbonate precipitation, temporary pond in the floodplain

table 1 continued.

Formation	FA	Facies	Lithology	Structures	Bedding	Fossil Content	Lateral and vertical relationships	Interpretation
Agua de los Pajaritos	C	Cn	Very light grey (N8) color nodular carbonate	Nodules at the base, faint discontinuous planar lamination at the top, laminae are 1 mm thick	Tabular, 0.8 m thick	-	Overlies Sh	Subaqueous calcium carbonate precipitation and pedogenic alteration, temporary pond in the floodplain
Monina	D	Sm	Yellowish grey (5Y8/1) color, fine-grained sandstone	Massive	Tabular to lenticular, 1.2-4.8 m thick	Plant remains (trunks) and rhizolits	Overlies Sh, Fm and Fl and underlies Sh and Fl	Tractive flows, deltaic system
		Sp	Yellowish grey (5Y8/1) color, pebbly sandstone	Planar cross stratification	Lentiform, 3.6 m thick	-	Overlies Fm	
		Sl	Grayish pink (5R8/2) color, poorly sorted, medium- to coarse- grained sandstone	Low angle lamination, lateral accretion	Tabular to lentiform, 0.3 m thick	-	Overlies and underlies Sh	
		Sr	Pale red (10R6/2) color, fine- to medium-grained sandstone	Ripple cross stratification, ripples: 0.5 cm thick and 3 cm spacing	Tabular, 0.25-1.2 m thick	-		
		Sh	Yellowish grey (5Y8/1) color, fine-grained tuffaceous sandstone	Horizontally laminated, laminae are 0.5-2 cm thick, clast lags	Tabular, 0.5-4.8 m thick	-	Underlies Sm	
		Fm	Yellowish grey (5Y8/1) color siltstone	Massive to nodular, nodules are 2 cm in diameter	Tabular, 0.7-2.4 m thick	Rhizohaloes, 1 cm in diameter		Suspension settle out from waning flows, incipient paleosol development in the delta plain
	E	Fl	Dark greenish grey (5GY4/1) color mudstone	Horizontal lamination, laminae are 1 mm thick and Fe concretions of 2 cm in diameter	Tabular, 0.1-3.6 m thick	-	Underlies Sp, Cm and Fm and overlies Fm and Cm	Suspension settle out, lacustrine system
		Cm	Very light grey (N8) color, carbonate	Massive	Tabular, 0.5 m thick	-	Underlies and overlies Fl	Subaqueous calcium carbonate precipitation in the lake margin
Hilario	C	Fm Fh	Greyish yellow green (5GY7/2), yellowish grey (5Y8/1), greenish grey (5Y6/1), olive grey (5Y4/1), pale brown (5YR5/2) siltstone	Massive, faint horizontal lamination, silicified patches and/or carbonate nodules of 5 cm in diameter, very light grey (N8) mottling and 2 cm in diameter, clast lags	Tabular, 0.07-7 m thick	Carbonaceous plant remains	Overlies Cn, Tf and underlies Cn, Tf and Cd	Suspension settle out from waning flows in the floodplain with carbonate rich ponds

table 1 continued.

Formation	FA	Facies	Lithology	Structures	Bedding	Fossil Content	Lateral and vertical relationships	Interpretation
Hilario	C	Cn	Very light grey (N8), brownish grey (5YR4/1) color, carbonate	Planar lamination to nodular, nodules of 4 cm in diameter	Lenticular, 0.6-1.2 m thick and laterally 1.5 m	Rhizolit	Overlies Fm-Fh and underlies Fm-Fh and Tf	Subaqueous calcium carbonate precipitation and pedogenic alteration, temporary pond in the floodplain, perhaps in crevasse splay deposit?
		Cd	Light olive grey (5Y 6/1) color, carbonate	Horizontal lamination, domal morphology, domes spacing is 5 cm and 2 cm thick, silicified	Tabular, 0.09-0.4 m thick		Underlies and overlies Sr	Subaqueous calcium carbonate precipitation, pond in the floodplain
		Tf	White (N9) color tuff	Massive	Tabular to lenticular, 0.25-3 m thick		Overlies and underlies Fm and Cn	Ash fall
	B	Gm	Pale yellowish orange (10YR8/6) color, poorly sorted, clast-supported, angular pebble- to cobble-intraformational breccia	Massive, matrix composed of fine-grained sandstone	Tabular, 0.6 m thick, erosive base	-	Overlies Fm	Debris flow
		St	Yellowish grey (5Y8/1) color, fine- to medium-grained to pebbly sandstone	Trough cross stratification, sets: 0.5 cm thick, cosets: 7 cm thick, pebbles are angular	Tabular, 0.8-2 m thick	-	Overlies and underlies Fm	Tractive flows, fluvial system
		Sr	Pinkish grey (5YR 8/1), light olive grey (5Y6/1) color, medium- to coarse-grained sandstone	Ripple cross stratification, spacing is 3-10 cm and thickness is 0.5-2 cm	Tabular, 0.6-1.2 m thick	-	Underlies Sh and Overlies Sh and Cd	
		Sh	Dusky yellow (5Y6/4) color, medium-grained sandstone	Horizontal lamination, laminae are 2 cm thick	Lenticular, 0.6-1.05 m thick, laterally 2.4 m	-	Overlies Sr and underlies Fm	
El Alcázar	C	Fl	Light olive gray (5Y6/1) color mudstone	Horizontal lamination	Tabular, 1.3 m thick	-	Overlies and underlies Sm	Suspension settle out from waning flows in the floodplain
		Cl	Brownish black color (5YR2/1), carbonate	Planar lamination, laminae are 0.5 cm thick	Tabular, 0.06 m thick	-	Overlies Sm and underlies Sh	Subaqueous calcium carbonate precipitation
	B	Sm	Very light grey (N8) color, well sorted, fine- to medium-grained, tuffaceous sandstone	Massive, rare flasser bedding	Tabular, 0.5-2.9 m thick	Plant remains (trunks)	Overlies Fl and Sr and underlies Cl and Sr	Tractive flows, fluvial system
		Sr	Greenish grey (5GY6/1), pinkish grey (5YR8/1) color, medium- to coarse-grained, arkosic to tuffaceous sandstone	Ripple cross lamination, ripples: 1 cm thick and 3 cm spacing	Tabular to lenticular, 0.9-9 m thick, erosive base	Plant remains (trunks)	Overlies Sh and Sm and underlies Sm	

facies association B (FA-B) that record tractive flows in a fluvial system (Table 1, Figs. 2, 3C). Massive siltstone beds (lithofacies Fm, Cn and Cm) overlays FA-B in a gradual transition recording subaqueous carbonate precipitation. Subjected to pedogenic alteration, most likely in temporary ponds in a floodplain subenvironment (Table 1, Figs. 2, 3D, E). These deposits have been interpreted as the synrift infill within the Sorocayense-Hilario sub-basin (Abarzúa, 2016).

The Agua de los Pajaritos unit is gradually overlain by the Monina Formation (Baraldo and Guerstein, 1984; Barredo and Stipanicic, 2002; Abarzúa 2016) comprising FA-D with planar-cross stratified sandstone, horizontally laminated sandstone, ripple-cross laminated sandstone, sandstone with low angle lamination and massive sandstone (lithofacies Sp, Sh, Sr, Sl, Sm and Fm) (Table 1, Figs. 2, 4A, B). These deposits are interpreted as tractive flows and suspension settle out from waning flows with incipient paleosol development in a deltaic subenvironment. The upper section of the unit presents FA-E with dark greenish mudstone with very fine lamination (lithofacies Fl) and massive carbonates (lithofacies Cm) interpreted as a combination of suspension settle out processes in the lake (Fl) and subaqueous calcium carbonate precipitation in the lake margin (Cm). The massive features of the carbonate fabric suggest alteration after deposition most likely due to subaerial exposure effect.

Upwards, the Hilario Formation gradually overlies the Monina Formation (Baraldo and Guerstein, 1984; Barredo and Stipanicic, 2002; Abarzúa, 2016) and is characterized by FA-B including clast supported conglomerates, trough cross-stratified sandstone, ripple-cross laminated sandstone and horizontally laminated sandstone (lithofacies Gm, St, Sr and Sh (Table 1, Figs. 2, 4C). FA-C gradually overlies FA-B with massive to faintly laminated siltstone, nodular and domal carbonate and white tuff (lithofacies Fh, Fm, Cn, Cd and Tf) (Table 1, Figs. 2, 4D, E). In this unit, this facies association differs from FA-C in the Agua de los Pajaritos unit in that carbonates present a varied macrofabric from domal (Cd) to nodular (Cn) recording different processes and an ash fall event is recognized. The deposits are interpreted as suspension settle out from waning flows in the floodplain, calcium carbonate precipitation occurred subaqueously with subsequent pedogenic alteration, therefore this subenvironment might represent temporary ponds in the floodplain with ash fall contribution. Sandstone and siltstone to fine conglomerate cover the lacustrine shale and are interpreted as deltaic mouth bars to low energy fluvial plains (Hilario Formation). At its top this sedimentary sequence includes white and green fallout tuffs and fine-grained tuffs, sometimes with siliceous replacement (Barredo, 2012).

The uppermost part of the Sorocayense Group is represented by the El Alcázar Formation (Table 1, Figs. 2, 5A, B) conformed by FA-C with lithofacies finely laminated mudstone (lithofacies Fl) and laminated carbonate (lithofacies Cl) interpreted as tractive flows in a fluvial system; and FA-B with ripple-cross laminated and massive sandstone (lithofacies Sr and Sm); and carbonate precipitation in ponds within the floodplain (Abarzúa, 2016). This unit unconformably overlies the synrift deposits and has been assigned to an early post-rift stage (Barredo, 2004).

3. Methods

Two high-resolution sedimentary logs were measured in two localities, Quebrada del Agua de los Pajaritos and Quebrada El Alcázar, and lithofacies identified as siliciclastic facies from coarse to fine-grained size and carbonate-dominated facies. Lithofacies code of Miall (1996) has been applied. Every carbonate rock level in the sedimentary logs was sampled including lateral variations within them, obtaining sixteen hand samples. Samples were named with an abbreviation of the formation plus a correlative number. These samples represent all of the limestones found in these rock successions. Thin sections of hand samples were done at the Laboratorio de Corte de Rocas at the Universidad Nacional de San Luis (UNSL) and were studied using a standard petrographic microscope (Olympus BX-51). Carbonate rocks petrographic classification follows criteria from Gierlowski-Kordesch (2010). The Rock Color Chart of the Geological Society of America (GSA) was used for color descriptions. The macrofabric study of the samples was done at the Laboratorio de Paleontología del Instituto Argentino de Nivología, Glaciología y Ciencias Ambientales (IANIGLA).

Criteria to differentiate primary carbonate from diagenetic carbonate phases included a thorough multiproxy study with petrography and

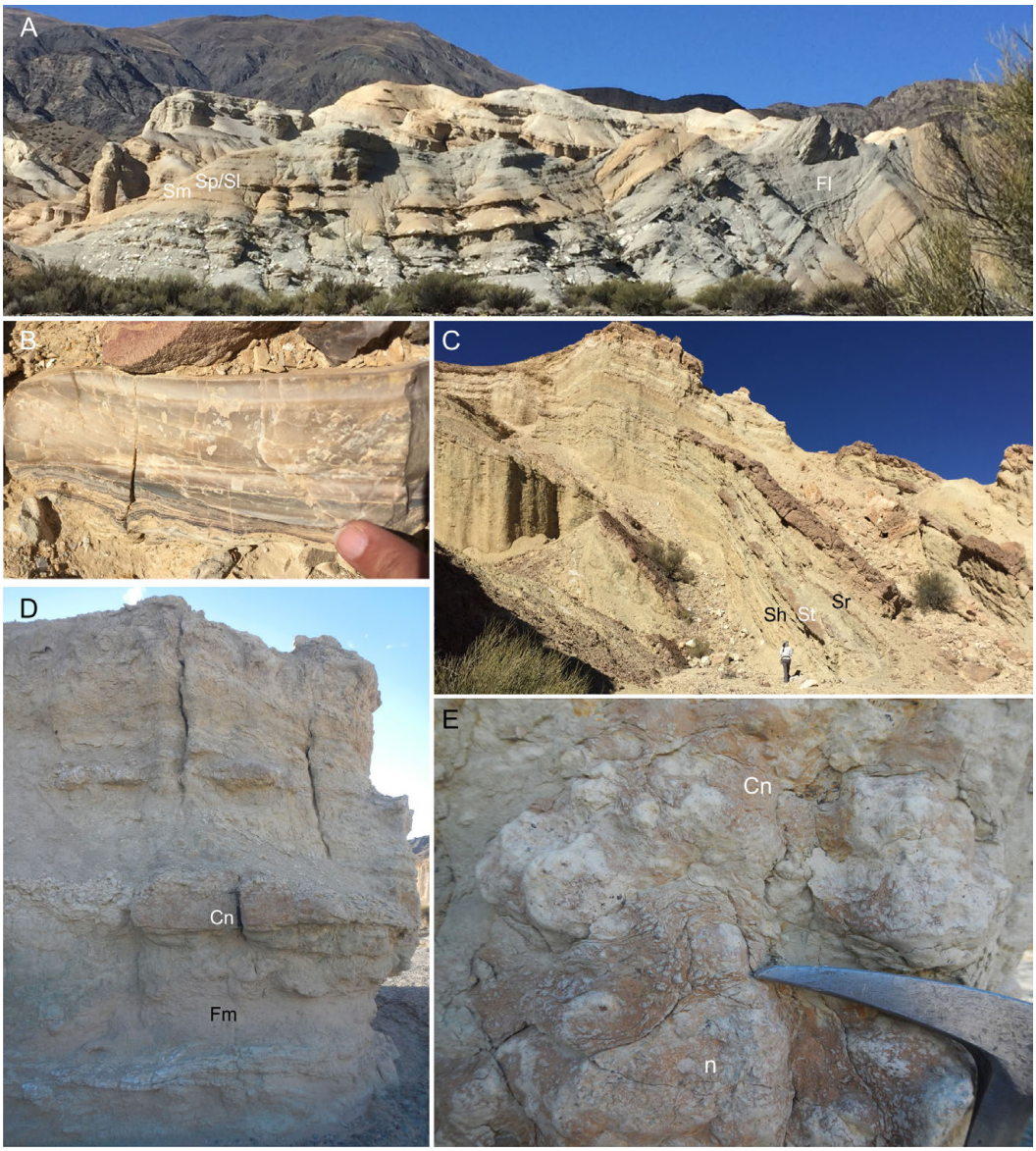

FIG. 4. Field photographs of the lithofacies and facies associations of the Monina and Hilario formations, Sorocayense Group. **A.** Outcrop view of the stratification of sandstones (yellowish color, Sm, Sp and Sl lithofacies) and very thick siltstones packages (greyish color, Fm lithofacies) of the Monina Formation. **B.** Detailed of a silicified massive to laminated siltstone of the Monina Formation. **C.** General view of the lenticular sandstones (brownish color, St, Sr lithofacies) interstratified with the tabular sandstones (yellowish and greenish colors, Sh), Person for scale is 1.7 m. **D.** Interstratified tabular Fm-Fl lithofacies (eroded, negative relief) with lentiform and pinch out Cn lithofacies (positive relief). Scale is 25 cm. **E.** Detail of a Cn lithofacies level showing spherical nodules (n) in a disrupted matrix. Hammer point for scale is 10 cm.

cathodoluminescence analysis of sixteen samples representing every carbonate layer found in the logs (Murphy *et al*., 2014; Parrish *et al*., 2019; Henkes *et al*., 2018; Benavente *et al*., 2019, 2021a, b). Those analyses led to the identification of different carbonate phases. Criteria to define diagenetic stages of continental carbonates follow Armenteros (2010).

Cold-cathodoluminescence (TECHNOSYN MKIII) was conducted at the Petrography and Cathodoluminescence Lab, Centro de Investigaciones

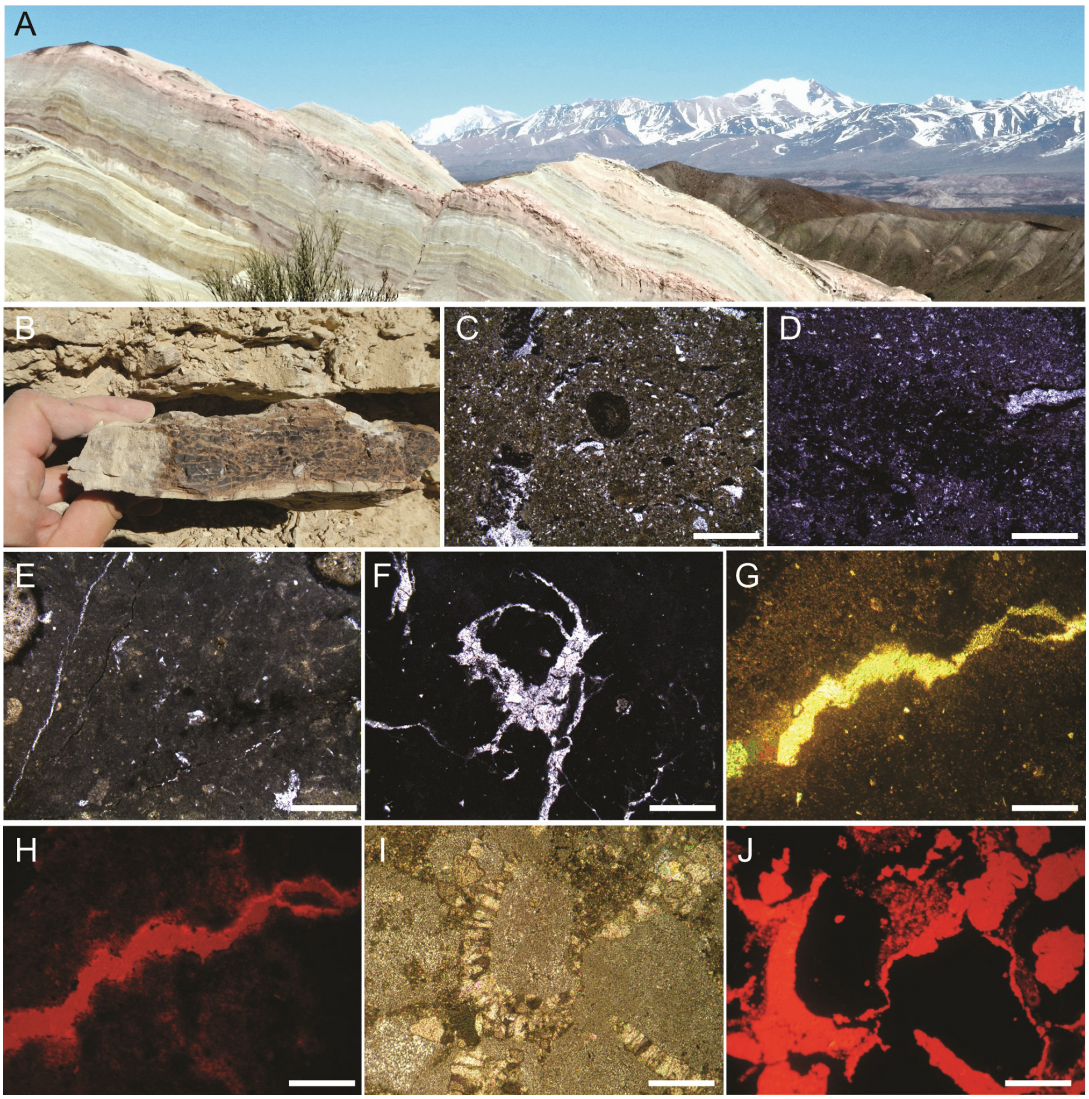

FIG. 5. Field photographs of the facies and facies associations of the El Alcázar Formation, Sorocayense Group and microphotographs of the Agua de los Pajaritos, Monina and Hilario carbonate thin sections. **A.** General view of the tabular sandstones dominated by tuff input of the El Alcázar Formation. **B.** Detail of Cl lithofacies with disrupted planar lamination. **C.** Microphotograph of the homogeneous micrite microfacies (Agua de los Pajaritos Formation) showing a clotted micrite matrix with circular concentric laminated structures interpreted as rhizolithes. Scale is 300 µm. **D.** Detail of a horizontal crack disrupting the matrix, filled by spar. Scale is 250 µm. **E.** Microphotograph of the homogeneous micrite microfacies (Hilario Formation) showing a clotted micrite matrix with diffuse circular micrite structures and vertical cracks. Scale is 250 µm. **F.** Detail of a circumgranular crack interpreted as disruption by rhizolithes. Scale is 100 µm. **G.** Detail of a vein under plane polarized light. Scale is 200 µm. **H.** Same vein as in G under cold cathodoluminescence showing zonation: the external fringe of the vein is bright luminescent while the interior of the vein is dull. Scale is 200 µm. **I.** Detail of the circular micrite structures under cross-polarize light with an external rim of blocky calcite. Scale is 50 µm. **J.** Same structures as in I under cold cathodoluminescence showing the blocky calcite with bright luminescence. Scale is 50 µm.

Geológicas (CIG) in La Plata, Argentina. For this purpose, 10-µm-thick thin sections were cut from each sample; they were double polished and then coated with resin (Marshall, 1988). Analytical conditions were 0.01 and 0.05 Torr vacuum with 14-19 Kv under 370-500 µA.

4. Results

4.1. Carbonate petrography and cathodoluminescence

Six microfacies have been identified in the carbonates of the Sorocayense Group (Table 2).

4.1.1.Homogeneous micrite

This microfacies has been identified in the carbonates of the Agua de los Pajaritos, Monina and Hilario formations. The matrix consists of homogeneous clotted micrite with dispersed circular micrite structures with concentric lamination of 250 to 625 µm of diameter (Fig. 5C, D, E) and carbonate intraclasts of 250 µm of diameter. The circular laminated structures are coated by a rim of blocky calcite of 25 µm wide and surrounded by crack systems of circumgranular cracks (Fig. 5F) and vertical cracks that bifurcate downwards and vary in size from 25 to 250 µm. These cracks are associated with reddish, brownish and black organic matter and filled by spar (Fig. 5D). Siliciclasts are angular to subangular quartz grains of 100 to 750 µm. Cements correspond to microspar, spar and microgranular silica (Table 2). This microfacies presents microstylolites and veins filled by spar in the carbonates of the Hilario Formation. Cathodoluminescence study shows that the veins are zoned with an external more luminescent zone and an internal dull zone (Fig. 5G, H). Blocky calcite coating the circular micrite structures presents medium luminescence (1,400 ppm Mn^{++}) (Fig. 5I, J) (Table 2).

Interpretation: The clotted micrite matrix suggests primary biogenic induced precipitation (cf. Dupraz *et al*., 2009; Benavente *et al*., 2015). The circular laminated micritic structures associated with circumgranular and vertical cracks are interpreted as rhizolites and the organic matter associated with the crack systems as cutans. These structures disrupting the fabric in a paleosol are interpreted as part of rhizobrecciation processes (cf. Freytet and Plaziat, 1982; Alonso-Zarza *et al*., 1992; Benavente *et al*., 2015). The presence of angular to subangular siliciclasts dispersed in the matrix indicates proximity to provenance area (Benavente *et al*., 2015). Non-luminescence of the carbonates of this facies points to no Mn content or either very low Mn content (17-25 ppm) combined with high Fe content (200 ppm or more). This suggests crystal cores with oxygen and therefore might indicate no significant burial (cf. Hiatt and Pufahl, 2014). The blocky calcite forming rims indicates a cementation stage in the phreatic zone (cf. Armenteros, 2010). The presence of different luminescent patterns and microstylolites found exclusively in the Hilario Formation carbonates indicates late mesogenesis probably linked to chemical compaction processes (cf. Brigaud *et al*., 2009).

4.1.2. Bioclastic micrite

This microfacies has only been found in the carbonate levels of the Hilario Formation. The matrix consists of homogeneous clotted micrite with dispersed disarticulated sparitic valves of 500 µm, articulated sparitic valves of 300 µm wide and 500 µm long (Fig. 6A), gyrogonites of 250 µm wide and 300 µm long and filamentous structures of 500 µm long with double wall. Gyrogonites consists of spar, and filamentous structures present an inner filament of silica and external wall replaced by spar, they are coated by micrite (Fig. 6B). Articulated valves have been micritized as well and the infill consist of spar (Fig. 6A). There is brownish organic matter dispersed in the matrix. Siliciclasts are angular quartz grains of 125 µm. Cements are micrite, spar, microgranular silica, and chalcedony in patches (Fig. 6C) and dispersed dolomite crystals (Fig. 6D). Chalcedony and dolomite crystals are 250 µm (Fig. 6C, D). There are vein systems with dull luminescence (1,200 and 1,600 ppm of Mn++) (Fig. 6E, F) (Table 2).

Interpretation: The clotted micrite matrix suggests primary biogenic induced precipitation (cf. Dupraz *et al*., 2009; Benavente *et al*., 2015). Gyrogonites correspond to the reproductive structures of charophyte algae, their presence indicates a soft substrate and a photic zone subenvironment probably with freshwater alkaline conditions. Filaments are interpreted as filamentous algae, possibly cyanobacteria. Both charophytes and cyanobacteria have been found abundantly in Middle Triassic deposits of the north Cuyana Basin (cf. Benavente *et al*., 2014, 2015). Articulated valves are identified as ostracod remains that have been found in association with charophytes and cyanobacteria before in Middle Triassic deposits of the north Cuyana Basin (cf. Benavente *et al*., 2014, 2015). Their presence indicates a subaqueous low energy subenvironment (cf. Bustos-Escalona *et al*., 2019). The presence of angular to subangular siliciclasts dispersed in the matrix indicates proximity

TABLE 2. SUMMARY OF THE PETROGRAPHY OF THE DIAGENETIC STAGES IDENTIFIED FOR THE CONTINENTAL CARBONATES OF THE SOROCAYENSE GROUP, SOROCAYENSE-HILARIO SUB-BASIN, CUYANA RIFT BASIN, ARGENTINA.

Formation	Microfacies	Petrography	Cement	Cathodoluminescence	Diagenetic stage	Interpretation
Agua de los Pajaritos	Homogeneous micrite	Veins	Microspar	Non-luminescent	Eogenesis	Biological processes, low Mn and high Fe in oxidizing microenvironment
Monina	Homogeneous micrite		-	Non-luminescent	Eogenesis	Biological processes, low Mn and high Fe in oxidizing microenvironment
Hilario	Homogeneous micrite		Micrite coating, microspar, microgranular silica, blocky calcite	Non-luminescent micrite. Blocky calcite with medium luminescence. Veins externally luminescent and internally dull.	Eogenesis-Late Mesogenesis	Biological processes. Cementation under high Mn content and moderate Fe content due to chemical compaction effect probably linked to shallow burial
	Bioclastic micrite	Veins	Micrite coating, spar, microgranular silica, chalcedony patches, dispersed dolomite crystals	Medium luminescence (1,200-1,600 ppm Mn++)	Late Mesogenesis	Cementation under high Mn content and moderate Fe due to chemical compaction effect linked to shallow burial
	Dolomicrite		Dolomite and microganular silica	Non-luminescent	Mesogenesis	
	Laminated micrite	Cellular clusters	Micrite coating, microspar, fibro-radial spar, microgranular silica	Non-luminescent micrite. External bright luminescent and internal non-luminescent cellular cluster	Eogenesis	Biological processes. Cementation under high Mn content and low Fe content due to inflowing fluids
	Oncolitic packstone		Micrite coating, blocky calcite	Non-luminescent micrite. Luminescent blocky calcite.	Late Eogenesis-Late Mesogenesis	Biological processes. Cementation under high Mn content and low Fe content due to diagenetic compaction effect
El Alcázar	Sparitic carbonate	Aggrading neomorphism	Microgranular silica	Non-luminescent	?	?

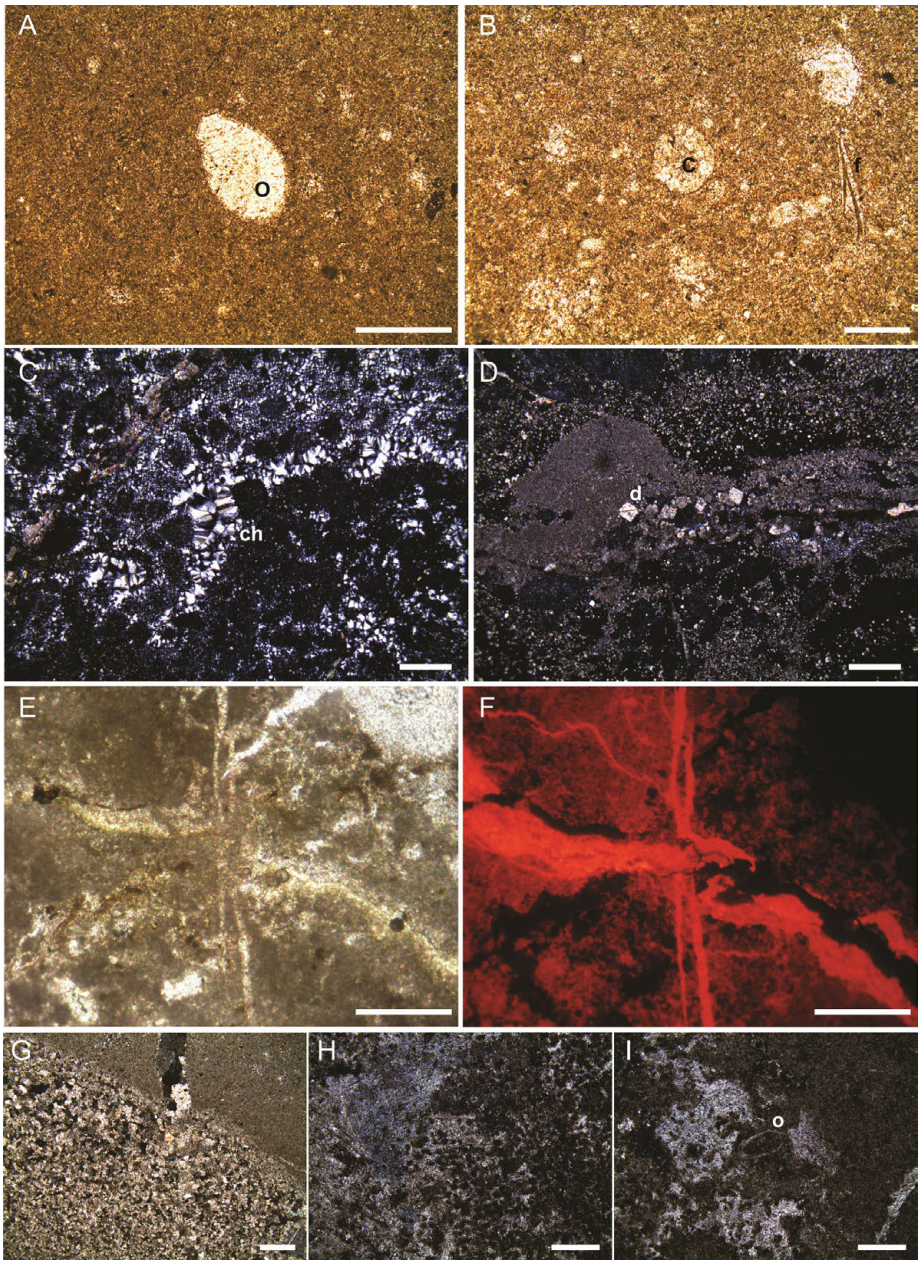

FIG. 6. Microphotographs of the Hilario carbonate thin sections. **A.** Bioclastic micrite microfacies showing clotted micrite with dispersed articulated valves interpreted as ostracods under plain polarized light. Scale is 450 µm. **B.** Bioclastic micrite microfacies under plain polarized light showing clotted micrite with dispersed poorly preserved gyrogonites and filamentous structures interpreted as Charophyte algae remains and filamentous algae remains respectively. Scale is 300 µm. **C.** Detail of the cements identified in the microfacies: microgranular silica and zebraic chalcedony under cross-polarized light. Scale is 300 µm. **D.** Detail of the cements identified in the microfacies: dispersed dolomite crystals of variable size under cross-polarized light. Scale is 300 µm. **E.** Detail of horizontal and vertical vein systems disrupting the micrite matrix under cross-polarized light. Scale is 300 µm. **F.** Same vein systems as in E under cold cathodoluminescence showing the horizontal veins are zoned with an external bright luminescent fringe and a dull interior whereas; the vertical veins present dull luminescence. Scale is 300 µm. **G.** Dolomicrite facies showing aggrading neomorphism. Scale is 300 µm. **H.** Laminated micrite microfacies with patches of circular to hexagonal structures with double external wall interpreted as vascular plant tissue remains. Scale is 150 µm. **I.** Detail of articulated overlapping valves interpreted as ostracod remains. Scale is 200 µm.

to provenance area (cf. Benavente *et al*., 2015). Therefore, this microfacies most likely represents shallow pond carbonate-rich subenvironments with microorganisms. The presence of dispersed dolomite crystals indicates isolated Mg-rich precipitation sites, since they are irregular a primary origin can be suggested (cf. Armenteros, 2010). In turn, this suggests a high Mg/Ca ratio for the subenvironment during precipitation (cf. García del Cura *et al*., 2001). Micrite coatings in bioclasts are interpreted as micritization processes that correspond to early diagenetic stages of eogenesis. The presence of veins with spar of dull luminescence indicates late mesogenesis probably linked to chemical compaction taking place after micritization.

4.1.3. Dolomicrite

This microfacies has only been found in the carbonate levels of the Hilario Formation. The matrix consists of homogeneous micrite, microspar and spar arranged in an aggrading increasing crystal size pattern (Fig. 6G). There are dispersed patches of black organic matter and vertical cracks disrupting the fabric. Cements are dolomite and microgranular silica. These cements are non-luminescent (Table 2).

Interpretation: The increasing crystal size pattern is interpreted as a neomorphism process that took place underwater with dissolution occurring contemporaneously to precipitation generating an increase in crystal size in one extreme of the microfacies only (cf. Bathurst, 1975; Armenteros, 2010). Non-luminescent cements indicate very low to low Mn content associated to a moderate or high Fe content, such conditions can be linked to oxidizing conditions that characterizes surficial dolomite precipitation (cf. Armenteros, 2010; Hiatt and Pufahl, 2014).

4.1.4. Laminated micrite

This microfacies has only been found in the carbonate levels of the Hilario Formation. The matrix consists of laminated clotted micrite. Laminae are crenulated and laterally continuous of 25 µm thick. There are patches of circular to hexagonal structures of 100 µm of diameter (Fig. 6H). Dispersed in the matrix there are articulated overlapping valves of 150 µm wide and 250 µm long and disarticulated valves of 200 µm long (Fig. 6I). The valves are sparitic and their infilling is micrite. The circular to hexagonal structures are massive and micritic with a double external wall, the inner layer of the wall is sparitic and they can present micrite coating. Organic matter is concentrated in the weak margins of the structures. There are also carbonate intraclasts of 125 µm and vertical cracks with associated reddish organic matter. Cements are microspar, fibro-radial spar, microgranular silica. The carbonate intraclasts are non-luminescent (Table 2).

Interpretation: The clotted micrite matrix suggests primary biogenic induced precipitation (cf. Dupraz *et al*., 2009; Benavente *et al*., 2015). Articulated and disarticulated valves are interpreted as ostracod remains. Their presence indicates a subaqueous low energy subenvironment (cf. Bustos-Escalona *et al*., 2019). The circular to hexagonal structures are doubtful. When observed in a more dispersed preservation they have circular shape and resemble coccoid algal or bacterial colonies (cf. Benavente *et al*., 2012, 2015). When they are preserved more organized and in connection to one another their shape is hexagonal and they resemble reticulate tracheid from plant tissue remains (cf. Bodnar and Falco, 2018). If they are indeed plant tissues, they indicate that their organic matter (OM) was partially replaced by calcium carbonate permineralization under rapid burial and low pressure conditions (cf. Scott and Rex, 1985) and OM was only retained in the weak margins of the structures. Micritization indicates an eogenesis diagenetic stage due to early precipitation of crusts around biogenic allochems (cf. Armenteros, 2010).

4.1.5. Oncolitic packstone

This microfacies has only been found in the carbonate levels of the Hilario Formation. The matrix is formed by microspar, spar, microgranular silica, chalcedony and dolomite. Carbonate grains are micrite oncolites spherical, oval, irregular in shape or fragmented and of 1,500 µm of diameter (Fig. 7A). The cortex consists of several concentric laminae and the nuclei are formed by bioclasts or replaced by spar or chalcedony. There are also spherical to irregular massive micrite structures of 500 µm of diameter. They are surrounded by an external layer of blocky calcite (Fig. 7B). There are articulated valves of 750 µm with syntaxial cement. Disrupting the fabric there are cracks of 1,250 µm. Under cold-cathodoluminescence, oncolites cortex shows alternating laminae of dark (Mn+2:~1,400-1,800 ppm) and light (Mn+2:~1,800-2,100 ppm)

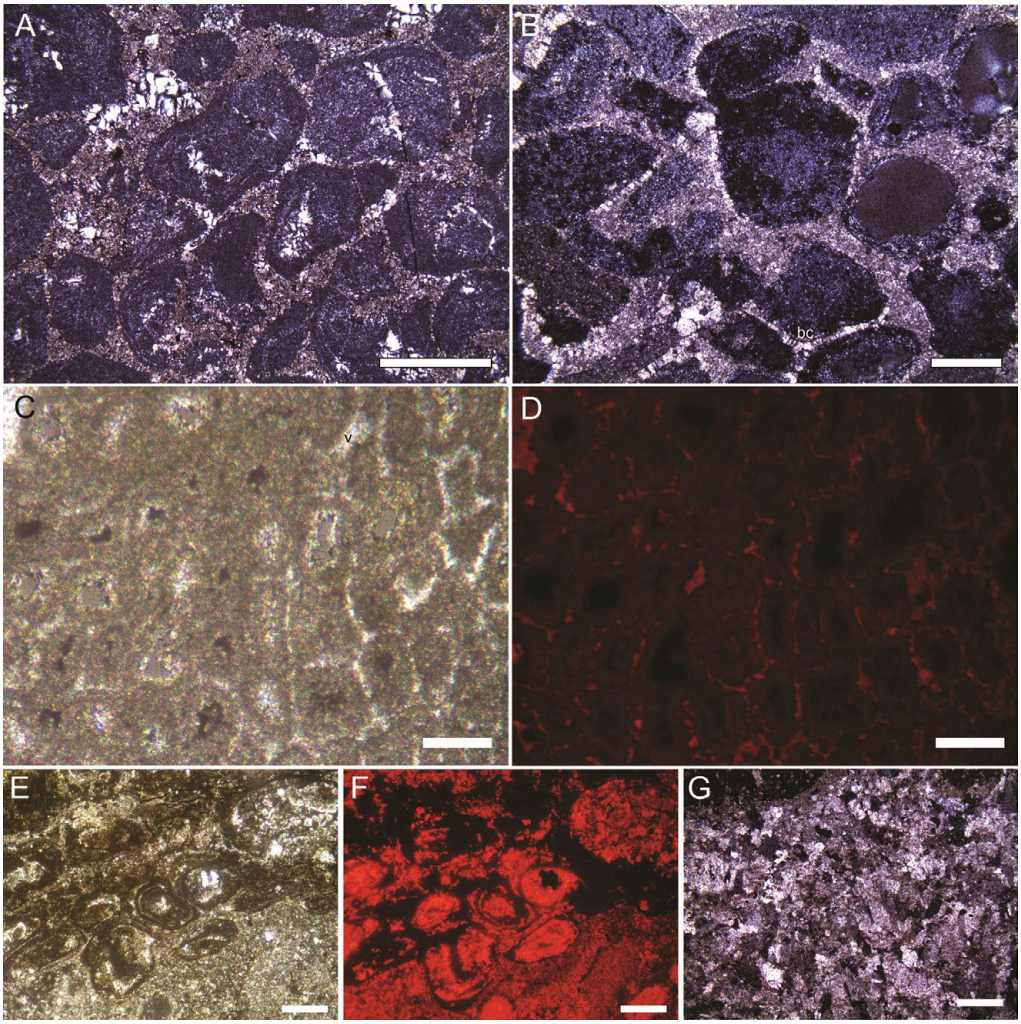

FIG. 7. Microphotographs of the Hilario and El Alcázar formations carbonate thin sections. **A.** Oncolitic packstone microfacies with complete or fragmented oncolites of variable morphology. Scale is 750 µm. **B.** Detail of massive micrite structures with an external blocky calcite rim. Scale is 750 µm. **C.** Detail of spherical to irregular structures under plane polarized light with empty centers, micrite and microspar rims and blocky calcite infilling the inter-structural spaces. Scale is 500 µm. **D.** Same microphotograph as in C under cold cathodoluminescence showing bright luminescent blocky calcite and dull luminescent spar and microspar. Scale is 500 µm. **E.** Detail of concentric laminae in the cortex of oncolites and nuclei replaced by spar under plane polarized light. Scale is 700 µm. **F.** Same oncolites as in E under cold cathodoluminescence showing non-luminescent nuclei and very bright luminescent cortex. Scale is 700 µm. **G.** Sparitic carbonate microfacies of the El Alcázar Formation with dominant cement replacement. Scale is 250 µm.

orange color (Fig. 7C, D). The nuclei are very low to non-luminescent. Blocky calcite is bright luminescent (Fig. 7E, F) (Table 2).

Interpretation: The different carbonate grains observed resemble a diagenetic trend in which the original component is interpreted to be the oncolites. Oncolites are interpreted as biogenically formed, probably linked to the microbial buildups of filamentous cyanobacteria that have been described in the bioclastic micrite microfacies. These microorganisms form biofilms over the substrate under low energy conditions but with higher energy conditions the biofilms are detached from the surface and move freely in the water body obtaining spheroidal or irregular structures. Similar oncolites and microorganism have been observed in other carbonate microfacies of the Middle Triassic

north Cuyana Basin (cf. Benavente *et al*., 2014, 2015). Fragmented and extremely ovoal oncolites are interpreted as the result of diagenetic compaction. The irregular and massive micrite structures are considered diagenetically altered oncolites that possibly underwent micritization. Different luminescence patterns indicate a range of diagenetic processes from late eogenesis to late mesogenesis.

4.1.6. Sparitic carbonate

This microfacies has only been found in the carbonates of the El Alcázar Formation. It is composed of spar mosaic with crystals of 250 μm. There are also microgranular silica patches and faint biogenic remains dispersed in the mosaic (Fig. 7G) (Table 2). The microfacies is non-luminescent.

Interpretation: the presence of significantly large spar crystals and faint biogenic remains suggests that spar cementation occurred obliterating the original carbonate microfabric. Sparitic cementation is considered a mesogenesis process (cf. Armenteros, 2010). Non-luminescence points to very low to low Mn combined with high Fe content (cf. Hiatt and Pufahl, 2014).

4.2. Relative chronology of diagenetic processes

This section summarizes the identified diagenetic phases in the Sorocayense Group microfacies. Based on petrography and cathodoluminescence we have stablished a relative chronological order of alteration of the carbonate primary fabric following the diagenetic environments proposed by Armenteros (2010).

4.2.1. Eogenetic

Very early diagenesis

Micritization. The very first process observed as result of diagenesis is the micritization of calcitic elements (spar) like the ostracod valves present in the bioclastic micrite microfacies of the Hilario Formation (Table 2, Figs. 1B and 8). This is a chemical process most likely due to pH changes in fluids in contact with the precipitating carbonates that cause frequent dissolution and re-precipitation (Blatt *et al*., 1980; Reid and Macintyre, 1998). Therefore, this process is part of the very early diagenesis and can occur simultaneously with primary carbonate precipitation.

Early diagenesis

Mechanical compaction. The following indicator of diagenesis observed is mechanical and it is identified as light compaction. This process is evidenced in the tangential contact between grains of the oncolitic packstone microfacies of the Hilario Formation (Table 2, Fig. 8), in one case the oncolites present sutured margins. This process is interpreted as early diagenesis (Bathurst, 1975).

4.2.2. Shallow mesogenetic

Cementation

Subsequent processes identified correspond to cementation. Three different types of cements have been identified.

Calcitic cement. It is composed by blocky calcite. It can present equidimensional or scalenohedral crystals of approximately 30 μm that occlude the porosity. This cement is luminescent and orange in color (Mn+2:1,400-1,800 ppm). It has been recognized in the homogeneous micrite microfacies of the Agua de los Pajaritos and Hilario formations, in the bioclastic micrite and laminated micrite microfacies of the Hilario Formation, and in the sparitic carbonate microfacies of the El Alcázar Formation (Fig. 1B). The cement has not been found in the Monina Formation carbonates (Table 2, Fig. 8). It postdate micritization and mechanical compaction and corresponds to diagenesis in the meteoric phreatic environment during late diagenesis (James and Choquette, 1990).

Sparitic cement. It is formed by a mosaic of drusyform crystals of 0.04 a 0.7 μm that occlude the porosity. It is found inside the intercrystalline porosity. Some crystals are zoned, one is non-luminescent and the other presents dull luminescence. This phase indicates late cementation in a reducing environment with high Fe+2 concentrations that cause low to non-luminescence. It has been identified in the oncolitic packstone microfacies of the Hilario Formation (Table 2, Fig. 8). This cement follows the calcitic cement and it is genetically linked to a first fracture formation event. The mechanical fracturing event would have allowed fluids with different chemical composition to interact with the precipitated carbonates generating cement precipitation in available pores.

Microsparitic cement. It presents moderate luminescence of light orange color and its genesis is linked to a second event of fractures. This cement is present in all the carbonate microfacies except in the El Alcázar Formation (Table 2, Fig. 8). This implies that this stage was common to the entire analyzed deposits suggesting a regional control such as tectonics.

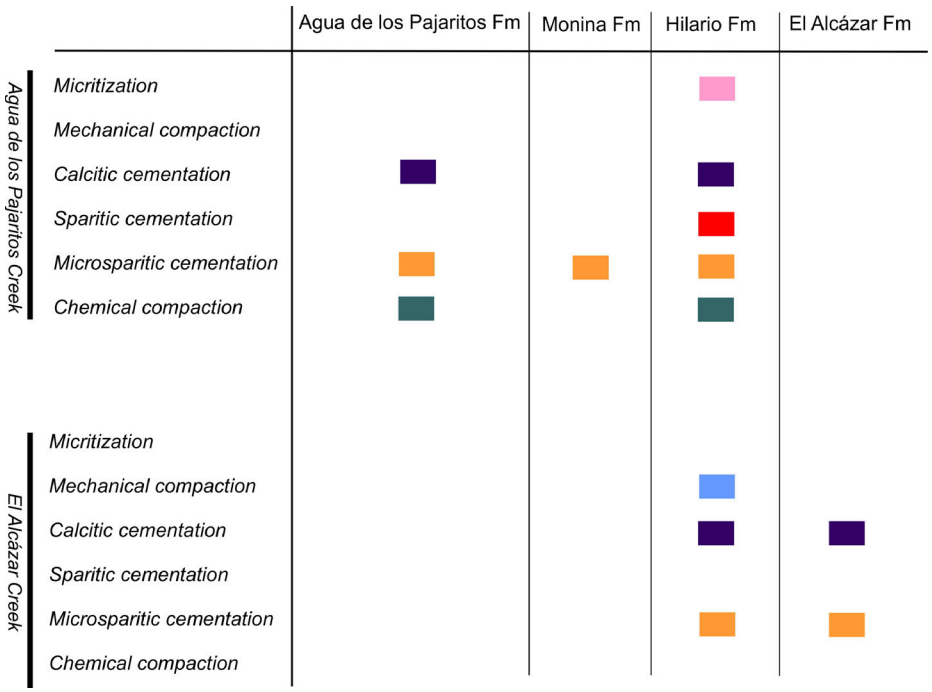

FIG. 8. Diagram showing the diagenetic stages identified and their distribution throughout the Sorocayense Group units.

4.2.3. Deep mesogenetic

Chemical compaction. It is characterized by the identification of microstylolites interpreted as the result of chemical compaction processes (Bathurst, 1975; Choquette and James, 1987). This has been observed in the homogeneous micrite microfacies of the Agua de los Pajaritos and Hilario formations at the Quebrada del Agua de los Pajaritos locality (Fig.1B). Also, the presence of crossed veins observed in the homogeneous micrite microfacies and the partial dissolution of bioclasts observed in the bioclastic micrite microfacies of the Hilario Formation along with the growth of dolomite crystals indicate late mesogenesis (Armenteros, 2010). This suggests that diagenetic effects were more pervasive at the Quebrada del Agua de los Pajaritos locality representing the flexural margin of the basin. This could be due to a paleohydrogeological effect by favoring the lateral inflow of meteoric waters.

5. Discussion

The tectonic configuration and stages of the rift are recorded by each unit deposited in the Sorocayense-Hilario sub-basin, and they have a direct link to the carbonate factory development in the subenvironments through time. In the initial stage of the synrift, when the sediments of the Agua de Los Pajaritos Formation were deposited, sediment supply exceeded the creation of accommodation. This was not the best scenario for the development of the carbonate factory (Benavente *et al*., 2021a). The most favorable conditions for the carbonate factory to develop occurred during the deposition of the Hilario Formation in which the accommodation and sediment supply were roughly at balance (Bohacs *et al*., 2000). During the deposition of the Monina Formation sedimentary rocks, accommodation surpassed water+sediment supply and therefore the carbonate factory could not be maintained, which is expressed by very few carbonate levels hosted in this unit (Fig. 2). During the El Alcázar Formation deposition the increased volcanic supply most likely was unfavorable for the carbonate factory to conspicuously develop.

All the carbonates analyzed in the lithostratigraphic units of the Sorocayense-Hilario sub-basin show features of very early and early diagenesis and a few record processes that indicate mesodiagenesis. The carbonate microfacies that present almost every diagenetic stage mentioned above are the ones of the

Hilario Formation representing the complete array of very early, early and late diagenesis (Fig. 8). This could be due to the fact that this unit is the one with most carbonate rocks. Since there are many different microfacies identified in these carbonate levels it is likely that a variety of diagenetic stages was recorded in such microfabrics since they would present different susceptibility to different diagenetic processes. Probably this is why, even though the Hilario Formation is not the base of the Sorocayense Group presents more diagenetic effects than the deposits of the Agua de los Pajaritos and Monina formations. When comparing the carbonates of the Hilario Formation in both studied localities, differences are notorious and the samples from the Quebrada del Agua de los Pajaritos present the most complex diagenetic evolution recording three diagenetic stages (very early, early and late diagenesis). This is interesting since that locality is the one linked to the most faulted section of the subbasin having been affected by several thrusts and folds (Fig. 1). This may suggest that tectonics was a main factor controlling diagenesis. Nevertheless, since the carbonates from other units of the Agua de los Pajaritos locality display a simpler diagenetic history, it is most likely that the susceptibility of the microfacies to diagenesis also played a significant role in the alteration processes. We interpret that tectonics, through the effect of faulting allowed circulation of fluids through the sedimentary succession and generated chemical compaction while being shallowly buried (Abarzúa, 2016). One significant feature to highlight, is that only one microfacies showed signs of mechanical compaction (Fig. 8), supporting previously proposed minor burial effect for the Sorocayense Group deposits (Abarzúa, 2016) and for the northern Cuyana rift Basin (Benavente *et al*., 2019). As it has been proposed by Abarzúa (2016) after infilling of the Triassic rift, sediments were shallowly buried by a thin sedimentary fill of the Cenozoic foreland basin in the northern part of the rift and then exposed only during Andean uplift episodes.

Another factor to suggest low burial effect is the presence of primary montmorillonite dominating clay assemblages of the fine-grained deposits of the Sorocayense Group (Tettamanti, 2020; Brigaud *et al*., 2009). This clay composition also has relevant implications for the diagenetic processes, since it generally supplies Mg which could be involved in dolomitization processes. Dolomite-rich deposits and interpretation of dolomitization are controversial for the record and even more for the continental carbonates record since modern analogues are scarce (Armenteros, 2010). However, the occurrence of dolomite in continental carbonate successions is widespread and moreover, also linked to primary biogenic processes mostly in lacustrine subenvironments (Sanz-Montero *et al*., 2006, 2008; Armenteros, 2010). Primary and very early diagenetic dolomite has been registered at modern permanent lakes (Anadón *et al*., 2000; Bustillo *et al*., 2002) and it can occur in different lake types such as ephemeral or meromictic. Such is the case of the Santa Clara Arriba lacustrine system of the adjacent Triassic Santa Clara sub-basin in Argentina (Benavente *et al*., 2021b) in which dolomite mosaics of 5 μm crystal size have been identified associated with organic matter and calcite spheroids and pyrite concretions. In that case, the geologic context and other proxies led to the interpretation that dolomite most likely precipitated as a primary phase in a Mg-rich meromictic lake (Benavente *et al*., 2021b).

In the case of the Hilario Formation, dolomite is found as dispersed crystals in microfacies that suggest a Ca-rich palustrine subenvironment. Other features such as subaerial exposure and weathering indicators, would suggest that most likely those dolomite crystals precipitated as a very early diagenetic stage. However, with current evidence it is not possible to discard a primary origin. Regarding the dolomicrite microfacies of this stratigraphic unit, the disposition in an aggrading neomorphism pattern suggests that dolomite is an early diagenesis replacement (Hay *et al*., 1968).

6. Conclusions

The continental carbonate rocks of the Sorocayense Group in the Sorocayense-Hilario sub-basin have been deposited and precipitated subaqueously in Ca-rich ponds of fluvial floodplains and in shallow lacustrine settings; they have undergone diagenetic processes that represent very early diagenesis, eogenesis and mesogenesis, whereas no evidence for telogenesis has been found. The more complex diagenetic evolution of the carbonates is found in the microfacies of the Agua de los Pajaritos locality, which is the most significantly thrusted and folded area of the sub-basin suggesting a tectonic control on some diagenetic processes.

Signs of mechanical compaction are scarce and, in agreement with previous tectonic studies in the sub-basin, indicate that the Triassic sedimentary column did not experience deep burial. The diagenetic study of these carbonates confirms those previous large scales analysis in a higher resolution and fine scale.

The presence of dolomite could be interpreted as primary in one microfacies and as the result of very early diagenesis in other. In any case, the supply of Mg for dolomite precipitation could be linked to montmorillonite clay dominated assemblages.

Akcnowledgements

Authors wish to thank Lic. González Pelegrí and Dr. Cuitiño for improving the manuscript through their revision; and Geól. Federico Ferri and Lic. Tomás Heredia for their assistance during field work. The study was funded by PICT2014-0489 (CAB).

References

Abarzúa, F. 2016. Estratigrafía, Análisis de Cuenca y Aspectos Exploratorios en el Extremo Norte de Cuenca Cuyana. Precordillera Occidental y Valle de Calingasta. Universidad Nacional de San Juan. Tesis doctoral (Unpublished): 225 p.

Alonso-Zarza, A.M.; Calvo, J.P.; García del Cura, M.A. 1992. Palustrine sedimentation and associated features, grainification and pseudomicrokarst, in the Middle Miocene (Intermediate Unit) of the Madrid Basin, Spain. Sedimentary Geology 76: 43-61.

Amos, A.J.; Quartino, B.J.; Zardini, R.A. 1971. Geología de la región Barreal-Calingasta, estratigrafía y estructura. *In* Estudio y exploración geológica de la Región de Barreal-Calingasta. Provincia de San Juan, República Argentina (Quartino, B.J.; Zardini, R.A.; Amos, A.J.; editors). Asociación Geológica Argentina, Monografía 1: 184 p.

Anadón, P.; Utrilla, R.; Vázquez, A. 2000. Use of charophyte carbonates as proxy indicators of subtle hydrological and chemical changes in marl lakes. Example from the Miocene Bicorb Basin, eastern Spain. Sedimentary Geology 133: 325-347.

Armenteros, I. 2010. Diagenesis of carbonates in continental settings. *In* Carbonates in continental settings, geochemistry, diagenesis and applications, developments in sedimentology (Alonso-Zarza, A.M.; Tanner, L.; editors). Elsevier 62: 61-151. Oxford.

Baraldo, J.A.; Guerstein, P.G. 1984. Nuevo ordenamiento estratigráfico para el Triásico de Hilario (Calingasta, San Juan). *In* Congreso Geológico Argentino, No. 9, Actas 1: 79-94, San Juan.

Barredo, S.P. 2004. Análisis estructural y tectosedimentario de la subcuenca de Rincón Blanco, Precordillera Occidental, provincia de San Juan. Buenos Aires, Argentina. Universidad de Buenos Aires. Thesis (Unpublished): 325 p.

Barredo, S.P. 2012. Geodynamic and Tectonostratigraphic study of a continental rift: The Triassic Cuyana Basin, Argentina. *In* Tectonics (Sharkov, E.; editor). Institute of Geology of Ore Deposits, Petrography, Mineralogy and Geochemistry (IGEM), Russian Academy of Sciences (Moscow): 99-130 p. Russia.

Barredo, S.P.; Stipanicic, P.N. 2002. El Grupo Rincón Blanco. *In* Léxico Estratigráfico de la Argentina, No. 3 (Stipanicic, P.N.; Marsicano, C.A.; editors): 870 p.

Barredo, S.P.; Chemale, F.; Ávila, J.N.; Marsicano, C.; Ottone, G.; Ramos, V.A. 2012. U-Pb SHRIMP ages of the Rincón Blanco Northern Cuyo rift, Argentina. Gondwana Research (21): 624-636.

Barredo, S.P.; Abarzúa, F.; Banchig, A. 2016. Nueva Propuesta Estratigráfica para el Triásico del Depocentro Agua de Los Pajaritos, Precordillera Occidental. Provincia De San Juan. *In* Jornadas de Geología de Precordillera, No. 3, Acta Geológica Lilloana 28: 52-57.

Bathurst, R.G.C. 1975. Carbonate Sediments and their Diagenesis: Developments in Sedimentology. Elsevier: 620 p. New York.

Benavente, C.A.; Mancuso, A.C.; Cabaleri, N.G. 2012. First occurrence of charophyte algae from a Triassic paleolake in Argentina and their paleoenvironmental context. Palaeogeography, Palaeoclimatology, Palaeoecology 363-364: 172-183.

Benavente, C.A.; D'Angelo, J.A.; Crespo, E.M.; Mancuso, A.C. 2014. Chemometric approach to Charophyte preservation (Triassic Cerro Puntudo Formation, Argentina): Paleolimnologic implications. Palaios 9: 449-459.

Benavente, C.A.; Mancuso, A.C.; Cabaleri, N.G.; Gierlowski-Kordesch, E.H. 2015. Comparison of lacustrine successions and their paleohydrologic implications in the two sub-basins of the Triassic Cuyana rift, Argentina. Sedimentology 62: 1771-1813.

Benavente, C.A.; Mancuso, A.C.; Bohacs, K.M. 2019. Paleohydrogeologic reconstruction of Triassic carbonate paleolakes from stable isotopes: Encompassing two lacustrine models. Journal of South American Earth Sciences 95. doi: https://doi.org/10.1016/j.jsames.2019.102292.

Benavente, C.A.; Mancuso, A.C.; Irmis, R.B.; Bohacs, K.M.; Matheos, S. 2021a. Tectonically conditioned

record of continental interior paleoclimate during the Carnian Pluvial Event: the Upper Triassic Los Rastros Formation, Argentina. Geological Society of America Bulletin 134 (1-2): 60-80.

Benavente, C.A.; Mancuso, A.C.; Bohacs, K.M. 2021b. Reconstructing paleoenvironmental conditions through integration of paleogeography, stratigraphy, sedimentology, mineralogy, and stable isotope data of lacustrine carbonates-an example from early Middle Triassic strata of southwest Gondwana, Cuyana Rift, Argentina. *In* Limnogeology: Progress, challenges and opportunities: A tribute to Beth Gierlowski-Kordesch (Rosen, M.R.; Park-Bousch, L.; Finkelstein, D.B.; Pla-Pueyo, S.; editors). Springer: 471-509. Switzerland.

Blatt, H.; Middleton, G.; Murray, R. 1980. Origin of Sedimentary Rocks (2nd Edition). Prentice Hall, Englewood Cliffs: 782 p. New Jersey

Bodnar, J.; Falco, J.I. 2018. Fossil conifer woods from Cerro Piche Graben (Triassic-Jurassic?), North Patagonian Massif, Río Negro Province, Argentina. Ameghiniana 55: 356-362.

Bodnar, J.; Iglesias, A.; Colombi, C.; Drovandi, J. 2019. Stratigraphical, sedimentological and palaeofloristic characterization of the Sorocayense Group (Triassic) in Barreal depocenter. Andean Geology 46 (3): 567-603. doi: http://dx.doi.org/10.5027/andgeoV46n3-3127

Bohacs, K.M.; Carroll, A.R.; Neal, J.E.; Mankiewicz, P.J. 2000. Lake-basin type, source potential, and hydrocarbon character: an integrated sequence-stratigraphic-geochemical framework. *In* Lake basins through space and time (Gierlowski-Kordesch, E.H.; Kelts, K.R.; editors). American Association of Petroleum Geologists 46: 3-34.

Bonati, S.; Barredo, S.P.; Zamora Valcarce, G.; Cervera, M.; Kowloksky, E. 2008. Análisis tectosedimentario preliminar del Grupo Barreal, cierre norte de la Cuenca Cuyana, provincia de San Juan. *In* Congreso de Exploración y Desarrollo de Hidrocarburos, No. 7, Actas: 409-420. Mar del Plata.

Borrello, A.V.; Cuerda, A.J. 1965. Grupo Rincón Blanco (Triásico San Juan). Comisión de Investigaciones Científicas. Provincia Buenos Aires, Notas: 2 (10): 3-20. La Plata.

Brigaud, B.; Durlet, C.; Deconinck, J.-F.; Vincent, B.; Thierry, J.; Trouiller, A. 2009. The origin and timing of multiphase cementation in carbonates: Impact of regional scale geodynamic events on the Middle Jurassic Limestones diagenesis (Paris Basin, France). Sedimentary Geology 222: 161-18.

Bustillo, M.A.; Arribas, M.E.; Bustillo, M. 2002. Dolomitization and silicification in low energy lacustrine carbonates (Paleogene, Madrid Basin, Spain). Sedimentary Geology 151: 107-126.

Bustos-Escalona, E.L.; Mancuso, A.C.; Benavente, C.A. 2019. Bioerosion on Spinicaudata shells from a freshwater paleolake (Triassic), Mendoza, Argentina. Palaios 34: 616-630.

Choquette, P.W.; James, N.P. 1987. Diagenesis 12. Limestone-3. The deep burial environment. Geoscience Canada 14 (1): 3-35.

Drovandi, J.M. 2020. La paleoflora triásica del Grupo Sorocayense, en la región de Hilario, cuenca de Barreal-Calingasta, provincia de San Juan. Universidad Nacional de La Plata. Thesis (Unpublished): 239 p.

Dupraz, C.; Reid, R.P.; Braissant, O.; Decho, A.W.; Norman, R.S.; Visscher, P.T. 2009. Processes of carbonate precipitation in modern microbial mats. Earth-Science Reviews 96: 141-162.

Freytet, P.; Plaziat, J.C. 1982. Continental carbonate sedimentation and pedogenesis. Late Cretaceous and Early Tertiary of Southern France. *In* Contributions to Sedimentology (Purser, B.H.; editorial) 12: 1-213.

García del Cura, M.A.; Calvo, J.P.; Ordóñez, S.; Jones, B.F.; Cañaveras, J.C. 2001. Petrographic and geochemical evidence for the formation of primary, bacterially induced lacustrine dolomite: La Roda 'white earth' (Pliocene, central Spain). Sedimentology 48: 897-915.

Gierlowski-Kordesch, E.H. 2010. Chapter 1 Lacustrine Carbonates. *In* Carbonates in Continental Settings: Facies, Environments and Processes, Developments in Sedimentology (Alonso-Zarza, A.M.; Tanner, L.H.; editors). Elsevier 61: 1-101. doi: https://doi.org/10.1016/S0070-4571(09)06101-9

Grover, G.Jr.; Read, J.F. 1983. Paleoaquifer and Deep Burial Related Cements Defined by Regional Cathodoluminescent Patterns, Middle Ordovician Carbonates, Virginia. The American Association of Petroleum Geologists Bulletin 67 (8): 1275-1303.

Hay, R.L. 1968. Chert and its sodium-silicate precursors in sodium carbonate lakes of East Africa. Contributions to Mineralogy and Petrology 17: 255-274.

Henkes, G.A.; Passey, B.H.; Grossman, E.L.; Shenton, B.J.; Yancey, T.E.; Pérez-Huerta, A. 2018. Temperature evolution and the oxygen isotope composition of Phanerozoic oceans from carbonate clumped isotope thermometry. Earth and Planetary Science Letters 490: 40-50.

Hiatt, E.E.; Pufahl, P.K. 2014. Cathodoluminescence petrography of carbonate rocks: application to understanding diagenesis, reservoir quality, and pore system evolution. *In* Cathodoluminescence and its application to geoscience: Mineralogical Association

of Canada (Coulson, I.; editor). Short Course Series 45: 75-96.

James, N.P.; Choquette, P.W. 1990. Limestone 2 the meteoric diagenetic environment. *In* Diagenesis (McIlreath, I.A., Morrow, D.W.; editors). Geoscience Canada, Reprint Series 4: 35-73.

Japas, M.S.; Cortés, J.M.; Pasini, M. 2008. Tectónica extensional triásica en el sector norte de la Cuenca Cuyana: primeros datos cinemáticos. Revista de la Asociación Geológica Argentina 63 (2): 213-222.

Legarreta, L.; Kokogian, D.A.; Dellape, D. 1993. Estructuración terciaria de la Cuenca Cuyana: ¿Cuánto de inversión tectónica? Revista de la Asociación Geológica Argentina 47: 83-86.

López Gamundí, O.R.; Espejo, I.; Conaghan, P.J.; Powell, P.J. 1994. Southern South America. *In* Permian-Triassic Pangean Basins and foldbelts along the Panthalassan margin of Gondwanaland (Veevers, J.J.; Powell, P.J.; editors). Geological Society of America, Memoir: 184 p.

Marshall, D.J. 1988. Cathodoluminescence of Geological Materials. London, Sydney, Wellington. Unwin Hyman: 146 p.

Miall, A.D. 1996. The Geology of Fluvial Deposits-Sedimentary Facies Basin Analysis, and Petroleum Geology. Springer: 582 p. Berlin.

Murphy, Jr.J.T.; Lowenstein, T.K.; Pietras, J.T. 2014. Preservation of primary lake signatures in alkaline earth carbonates of the Eocene Green River Wilkins Peak-Laney Member transition zone. Sedimentary Geology 314: 75-91.

Ottone, G.E.; Macino, J.; Erra, G.; Barredo, S.; Larriestra, F. 2019. Palynology, Palynofacies and Geochemistry on the Triassic Casa Piedra Formation, Rincón Blanco Group, Argentine Precordillera: Depositional Environment and Hydrocarbon Potential. Ameghiniana 56: 319-335.

Parrish, J.T.; Hyland, E.G.; Chan, M.A.; Hasiotis, S.T. 2019. Stable and clumped isotopes in desert carbonate spring and lake deposits reveal palaeohydrology: A case study of the Lower Jurassic Navajo Sandstone, south-western USA. Sedimentology 66 (1): 32-52.

Ramos, V.A. 2000. The Southern central Andes. *In* Tectonic Evolution of South America (Cordani, U.G.; Milani, E.J.; Thomaz, F.A.; Campos, D.A.; editors). *In* International Geological Congress, No. 31, Actas: 561-604. Rio de Janeiro.

Ramos, V.A.; Kay, S.M. 1991. Triassic rifting and associated basalts in the Cuyo Basin, central Argentina. *In* Andean magmatism and its tectonic setting (Harmon, R.S.; Rapela, C.W.; editors). Geological Society of America Special Paper 265: 79-91.

Reid, R.P.; Macintyre, I.G. 1998. Carbonate recrystallization in shallow marine environments: a widespread diagenetic process forming micritized grains. Journal of Sedimentary Research 68 (5): 928-946.

Sanz-Montero, M.E.; García del Cura, M.A.; Rodríguez-Aranda, J.P. 2006. Facies dolomíticas de sistemas lacustres miocenos en las cuencas del Duero y de Madrid. Rasgos indicativos de su origen microbiano. GeoTemas 9: 205-208.

Sanz-Montero, M.E.; Rodríguez-Aranda, J.P.; García del Cura, M.A. 2008. Dolomite-silica stromatolites in Miocene lacustrine deposits from the Duero Basin, Spain: The role of organotemplates in the precipitation of dolomite. Sedimentology 55: 729-750.

Scott, A.C.; Rex, G. 1985. The formation and significance of Carboniferous coal balls. Philosophical Transactions of the Royal Society of London B 311: 123-137.

Spalletti, L.A. 2001. Modelo de sedimentación fluvial y lacustre en el margen pasivo de un hemigraben: el Triásico de la Precordillera occidental de San Juan, República Argentina. Revista de la Asociación Geológica Argentina 56 (2): 189-210.

Stipanicic, P.N. 1972. Cuenca triásica de Barreal. *In* Geología Regional Argentina (Leanza, A.F.; editor). Academia Nacional de Ciencias: 537-566.

Stipanicic, P.N. 1979. El Triásico del Valle del río Los Patos, Provincia de San Juan. *In* Simposio de Geología Regional Argentina, No 2, Academia Nacional de Ciencias, Actas: 695-744. Córdoba

Tettamanti, M. 2020. Sistema Petrolero de las Unidades Triásicas del Grupo Sorocayense al Norte de Barreal (Provincia de San Juan) y Respuesta Teórica de la Formación El Alcázar a los Perfiles Eléctricos, Universidad de Buenos Aires. Thesis (Unpublished): 119 p.

Uliana, M.A.; Biddle, K.T. 1988. Mesozoic-Cenozoic paleogeographic and paleodynamic evolution of southern South America. Revista Brasileira de Geociências 18: 172-190.

Manuscript received: January 28, 2022; revised/accepted: December 5, 2022; available online: January 31, 2023.
Editorial handling: Luis Lara.